Nasrin Haacke, Eva Paton

Impact-based classification of extreme rainfall events using a simplified overland flow model

Impact-based classification of extreme rainfall events using a simplified overland flow model

Authors: Nasrin Haacke[a*1] and Eva Paton[a]

[a]*Ecohydrology and Landscape Evaluation, Institute of Ecology, Technical University Berlin, Berlin, Germany*

Corresponding author: nasrin.haacke@bam.de

Second author (Eva Paton): eva.paton@tu-berlin.de

Biographical notes:

Nasrin Haacke: ORCID: 0000-0001-9065-729X; LinkedIN: Nasrin Haacke (https://www.linkedin.com/in/nasrin-haacke-b5207518b)

Eva Paton: ORCID: 0000-0002-5619-9958

[1] Current affiliation: Corrosion and Corrosion Protection, Safety of Structures, Federal Institute for Materials Research and Testing, Berlin, Germany

Impact-based classification of extreme rainfall events using a simplified overland flow model

Abstract

In this study, we present a new approach to rainfall classification that uses a simplified overland flow model to facilitate impact assessments of heavy rainstorms. Conventional rainfall classification approaches using peak intensities or rainfall sums can lead to misjudgements of the impact of rainfall event, as they do not explicitly consider the potential of rain to generate and sustain substantial amounts of overland flow on typical sealed, urban surfaces. The new method of impact-based rainfall classification proposed here comprises three steps: Identification of rainfall events from high-resolution time series, computation of overland flow depths for each event, and impact-based classification of rainfall events as a function of the magnitude of overland flow. The accuracy of this approach was evaluated with respect to its ability to describe seasonal and annual occurrences of and variations in rainstorm impacts for high-resolution series at three different urban stations in Germany.

Keywords: flow depth, impact assessment, overland flow, urban flooding, rainfall classification

1. Introduction

Urban pluvial floods are caused by extreme rainstorms, with rainfall rates exceeding the capacity of urban drainage systems, and causing severe damage to urban infrastructure (Rözer et al. 2021). They are seen by many as invisible hazards (Forzieri et al. 2018; Jacobs et al. 2018; Moftakhari et al. 2017; Suarez et al. 2005), as they can often strike with little warning in areas with no recent record of flooding. The instances of pluvial flooding are rising due to a combination of global climate change, urbanisation, and a lack of investment in sewer and drainage infrastructure (Westra et al. 2014). Although many modelling software packages are available to simulate pluvial flooding in urban catchments (e.g. InfosWorks ICM (Innovyze 2020), SWMM (Rossman 2004), MOUSE (DHI 2000)), and many methods exist to describe the underlying hydrological processes (c.f. Salvadore et al. 2015), predicting the extent and severity of pluvial floods remains challenging. This is due to an incomplete understanding of the interactions between urban and natural hydrological systems, as well as the high degree of uncertainty (Salvadore et al. 2015).

Local information about urban drainage systems, topographic data, land use and soil moisture preconditions, and precipitation data with high spatial and temporal resolutions are needed to realistically reproduce complex hydrological processes. However, considering that it is time-consuming and costly to develop and run hydrological models, and- perhaps most decisively, the paucity of available data- the utility and applicability of such models to urban pluvial flooding remains limited. In recent years, the improvement of geographic information systems (GIS) and the availability of remote sensing data at higher resolutions have helped to link hydrologic processes and topography so that we may finally identify and map areas that are the most prone to flooding (Di Salvo et al. 2017). For example, a topography-based urban flooding index, the topographic wetness index (TWI), was developed and has increasingly been applied to urban settings via the Blue Spots method; this approach is focused specifically on identifying the surface depressions that are most prone to fill during high-intensity storms (Balstrøm and Crawford 2018).

While there has been great progress in the representation of surface characteristics, it is still common to represent rainfall events by design rainfalls with characteristics based on conventional rainfall classifications using time-aggregated data. For pluvial flooding, the focus has only been on extremes selected by either a percentile approach (99th and 95th percentiles (Brieber and Hoy 2019; Jacobeit et al. 2017; Schär et al. 2016 and citations therein)) or on events exceeding a certain threshold (peak-over-threshold method; (Acero et al. 2011; Agilan et al. 2021; Anagnostopoulou and Tolika 2012; Beguería et al. 2011; Haacke and Paton, 2021), both of which are based on averaged intensities; the most commonly used intensities are mm/1 h, mm/6 h, and mm/24 h. However, recent studies have shown that averaged rainfall intensities do not accurately represent the specific hydrography of extreme rainfall events and lead to the over-or underestimation of rainfall characteristics and to an incomplete understanding of the overland flow generated (as discussed in detail by Dunkerley 2020). A better approach would be to consider the actual lengths of rainfall events as event characteristics, such that the precipitation amount, mean rainfall rate, surface runoff volume and flow depth generated are defined in relation to it (Dunkerley 2008). The most intense periods of rainfall within a given event are thought to affect the flux, depth of overland flow, and infiltrability in different ways; for instance: a late peak event, shows higher runoff ratios and lower infiltration depths than an early peak event (Dunkerley 2017). The rainfall pattern (also termed ‘event profile’, which is defined as the time-varying sequence of rainfall intensities, including any intermittency) heavily controls the amount of infiltration and runoff (in addition to surface characteristics).

Recent studies have critiqued the fact that little attention has been paid to events resulting in low levels of flooding (Moftakhari et al. 2018). Such events are often thought to be less harmful; however, they are still able to generate substantial overland flow, leading to minor to moderate flooding, which may be amplified in highly sealed urban environments. Compared to extreme pluvial flooding, these events do not pose significant threats to public safety or cause major property damage; nevertheless, they can disrupt daily activities, add strain to infrastructure systems, and cause minor property damage (Moftakhari et al. 2018). They also trigger diffuse pollution transport processes on urban surfaces (Paton and Haacke 2021). Hence, we argue that rainstorm events should be evaluated and classified by their potential to generate overland flow on urban surfaces and not exclusively by their average or maximal intensities. We suggest applying an approach that is commonly used in soil erosion studies, especially on rural hillslopes, where overland flow depth has been successfully used to evaluate the impact of heavy rainfall on the incipient motion of unconsolidated sediments and adsorbed nutrients or pollutants (Abrahams et al. 1998; Parsons and Stromberg 1998; Yuan et al. 2019). The goal of this study was to present a new rainfall classification method based on the potential of individual rainstorm events to generate and sustain overland flow, defined as flow depth per time unit, on a simplified urban model surface, considering fluctuations in intensity and intermittency to represent rainstorm characteristics as accurately as possible. To illustrate the potential of the proposed method, it was additionally compared to a conventional method. We then applied this method to three stations across Germany to demonstrate its ability to describe the seasonal and annual occurrence of and variations in rainstorm impacts using high resolution data compiled over the last three decades.

2. Impact-based rainfall classification method

The new method for impact-based rainfall classification proposed here comprises three consecutive steps: rainfall event delineation, overland flow depth computation for each event, and impact-based classification of rainfall events as a function of overland flow. For event delineation, individual rainfall events were derived from continuous, long-term, high-resolution rainfall series with a temporal resolution of at least 10 min using a fixed inter-event time (IET). The overland flow depth generated by the delineated rainfall events was calculated for a typical urban sealed surface and used as an indicator of the magnitude of surface runoff and pluvial flooding. For impact-based classification, the same fixed flow depth thresholds were used to classify individual rainfall events according to the flow depth they were able to generate and sustain for a specific period of time. The method was applied and evaluated for three stations across a south-north transect through Germany (Würzburg, Potsdam, Hamburg); interim results were shown for the station Würzburg for illustration only.

2.1 Event delineation

Individual rainfall events were delineated from continuous rainfall time series with a 10-min time step or higher. Rain data of less than 0.1 mm per 10 min were disregarded, as they were considered artefacts of condensation or funnel drainage at the end of events and increased their duration while minimally increasing the rainfall depth (Gaál et al. 2014). To extract rainfall events, an IET of one hour was used to define rainless intervals between rainfall events (Fig. 1a), which was considered short enough to capture convective rainstorms events in the study region. For different climatic settings, the IET might have to be adjusted to identify typical IETs, as reviewed here by Dunkerley (2008).

Each delineated rainfall event was characterised and visualised by four summary values in a multi-dimensional scatterplot containing information on total rainfall depth (P), peak intensity, mean intensity and event duration (D). In particular, the last three characteristics represented critical drivers of overland flow (Fang et al. 2012; Sen et al. 2010) but have often been neglected or averaged in recent rainstorm classifications (Jo et al. 2020; Yoo and Park 2012). As an example of the delineation and characteristics of rainfall events, Figure 1b shows 105 delineated events for a rainfall series of the station Würzburg in Germany.

Figure 1

2.2 *Overland flow model*

An overland flow model after that of Scoging (1992) was used to calculate the flow depth as an indicator of the magnitude of surface runoff for a typical asphalt street surface for each delineated rainfall event (Fig. 2). The flow depth was chosen as an indicator of the impact of rainfall events, as it was successfully employed in a previous study (Yuan et al. 2019) as a proxy for incipient motion in unconsolidated sediments. The magnitude of the flow depth indicated that a significant amount of overland was generated, resulting in pluvial flooding and the redistribution of pollutants.

Figure 2

The overland flow model was based on a one-dimensional kinematic approximation of the dynamic St. Venant equation for the computation of flow depth. The continuity equation is given by:

$$\frac{\partial D(x,t)}{\partial t} + \frac{\partial q(x,t)}{\partial x} = ex(x,t) \qquad (1)$$

where q is the discharge per unit width [$mm^2 s^{-1}$)], D is the flow depth (mm), and ex is the rainfall excess [mm s^{-1}].

Equation (1) can be expressed in finite-difference form, where Δt time is increment in seconds:

$$\frac{D(x,t) - D(x,t-\Delta t)}{\Delta t} + \frac{q(x,t-\Delta t) - q(x-\Delta x, t-\Delta t)}{\Delta x} = ex(x, t-\Delta t) \qquad (2)$$

Rearranging, and solving for *D(x, t)*, the unknown:

$$D(x,t) = (ex(x,t)\Delta t) + D(x, t-\Delta t) + \frac{\Delta t}{\Delta x}[q(x-\Delta x, t-\Delta t) - q(x, t-\Delta t)]. \qquad (3)$$

Initially depth at $t = t_0 + \Delta t$ is determined entirely by *ex(x,t)* since inflow discharge is zero.

The infiltration rate, interception and depression storage of a typical sealed urban surface were assumed to have constant values as given in Table 1, derived from a recent review after (Rammal and Berthier 2020) and from terrestrial laser scan experiments on sealed surfaces by Nehls et al. (2015). The flow velocity v was calculated using the Darcy-Weisbach flow equation in infinite form:

$$v(x,t) = \sqrt{\frac{8\mathrm{g}D(x,t)s(x)}{ff(x,t)}} \qquad (4)$$

and

$$q(x,t) = D(x,t)\, v(x,t) \qquad (5)$$

where v is the flow velocity [$mm^2 s^{-1}$]), g is the gravitational constant [mm/s^2], s in the sine slope gradient [m/m] and *ff* in the Darcy-Weisbach friction factor [-].

Rainfall excess ex [mm s^{-1}] was defined as the amount of rainfall at a given time that could not infiltrate the surface and thus exceeded the interception and depression storage capacities:

$$ex(x,t) = \; r(x,t) - i(x,t) - loss(x,t) \qquad (6)$$

where r is the rainfall intensity [mm s^{-1}], i is the infiltration rate [mm s^{-1}], and *loss* is the loss due to interception and depression storage [mm s^{-1}]; once the loss storage is filled during a rain event, the loss term is set to zero.

The model street surface was represented by a 100-metre long and 10-metre wide model domain (total area = 1000 m^2), with a low slope and high degree of sealing; thus, the surface had a low infiltration rate and small interception and depression storage. Table 1 gives some typical parameter values for the street surfaces. The model time step was set to 10 s to ensure computational stability.

Figure 3 shows example outputs of the overland flow model for rainfall events with very low intensities (drizzle) and medium intensities over long periods (continual rain), resulting in no or minimal overland flow, as well as for rainfall events with high intensities of convection that generated substantial overland flow.

Table1

Figure 3

2.3 Impact-based classification of rainfall events

Most delineated rainfall events did not generate any overland flow, as their rainfall intensity and/or durations were too small (Fig. 3a & c); therefore, most rainfall either infiltrated or filled the interception and depression storage. Using this classification approach, the remaining rain events that generated and sustained certain overland flow depths over a specific time were categorised into four classes if severity. The severity of the impact that caused pluvial flooding and pollution transfer was defined with fixed thresholds for the flow depths (low, medium, high, or very high) and a specific minimum flow duration. When selecting a minimum flow duration, it should correspond to the temporal resolution of the rainfall series to avoid any artefacts of downscaling.

Figure 4 shows the process by which rainfall events were classified according to their ability to generate significant overland flow, and the simulated hydrographs of flow depths from multiple delineated rainfall events (Fig. 4a) are classified into four impact categories with flow depths of 1 to > 4 mm for at least 10 min (Fig. 4b).

Figure 4

2.4 Data requirement and test stations

Our classification method required the use of high-resolution rainfall data, with a temporal resolution of at least 10 min. The method was tested with rainfall data collected at intervals of 1 and 10 min and, a lower resolution is not advised because as time-averaged rainfall intensities will result in an incorrect reproduction of flow depth rates. High-quality time series of climate stations in Würzburg (ID = 5707), Hamburg (ID = 1975) and Potsdam (ID = 3987) (Climate Data Centre) were used to evaluate and present the classification method. Hamburg is located on the northwest coast, Potsdam in the north-western lowlands, and Würzburg in the central low-elevation mountains of Germany. The datasets covered a period of three decades from 1990 to 2020 (1993 – 2020 for Potsdam) and were selected because of their availability and high quality.

3 Evaluation of impact-based rainfall classification method

3.1 Evaluation of event delineation

The main challenge facing event delineation methods for rainfall series is the identification of the minimum number of hours with no or negligible rainfall to separate the time series into individual events. According to a review by Dunkerley (2008), the duration of the IET can range widely – from 3 min to 24 h for different seasons and climatic settings – thus, regional analyses of the optimal IETs are essential. Three different statistical approaches exist to identify the dry periods between two rainfall events: autocorrelation analysis (AutoA), average annual number of events analysis (AAEA) and coefficient of variation analysis (CVA). In AutoA, events are delineated by finding the IET at which the autocorrelation coefficient is no longer significantly different from zero, such that the rainfall event can be regarded as independent (Wenzel and Voorhees 1981). In AAEA, the IET is defined based on the average number of events annually, wherein an increasing IET is accompanied by a decrease in the average number of events. Finally, in CVA, it is assumed that IETs are represented well by an exponential distribution (Adams and Papa 2000; Restrepo-Posada and Eagleson 1982).

All three approaches were tested for the period from 1990 – 2020 for the study stations Würzburg, Potsdam and Hamburg using the '*IETD' package* (Duque 2020) in R version (4.1.1; R Core Team 2020). While the AAEA approach only presented the influence of potential IETs on rain event selection, the AutoA and CVA approaches calculated IETs between 1h23min – 2h35min and 13h42min – 17h30min at a significance level of 10% for the whole period, respectively. Smallest IETs were achieved in summer season (AutoA: 50min – 1h35min, CVA: 10h18min – 15h18min), longest IETs in winter (AutoA: 2h – 8h, CVA: 14h15min – 20h). In comparison, the CVA approach calculated much longer IETs for both the entire period and individual seasons.

Considering the wide ranges stemming from different delineation methods, no "correct" value for IET can be extracted. Restrepo-Posada and Eagleson (1982) and Dunkerley (2010) found that a longer IET may prove helpful in ensuring the identification of subsequent independent events. However, it adversely affects event properties, such as the duration and intensity of short-duration, convective rainstorms, which are known to occur mostly in the summer months in the study area (Haacke and Paton 2021).

Based on the derived IET specifically for the summer season by using AutoA (Fig. 5), an IET of 1 h was considered the most appropriate IET to ensure the detection of shorter events and used for further analysis. In total, 2969 events for Würzburg, 4304 events for Hamburg, and 2747 events for Potsdam were delineated for the study period 1990 – 2020.

Figure 5

3.2 Evaluation of the overland flow model

Computed flow depths depend strongly on the size of the model domain: the larger the model area, the higher the maximum flow depth. Figure 6 shows the exponential development of maximal flow depth with increasing model size for several delineated rainfall events from Würzburg Station, where the rainfall maxima ranged from 1 – 14 mm/10min. Maximum flow depths varied greatly between 1.7 and 24.9 mm, 0.5 and 6.4 mm, 0.3 and 2.9 mm, and 0.1 and 1.4 mm for a model size of 1.000.000 m^2 (edge length dx = 1000 m), 10.000 m^2 (dx = 100 m) 1.000 m^2 (dx = 31.62 m), and 100 m^2 (dx = 10 m), respectively. To represent an accurate size and to have reasonable computing times, we chose a model size of 1000 m^2, which was represented by 10 cells lined up and dx = 10 m.

The time series from Würzburg Station from 1990 – 2020 was chosen as an example, and the overland flow model was used to compute runoff depths for all 2969 delineated rainfall events (Fig. 4b). More than two-thirds of the events (71%) did not generate any overland flow, while ~29% generated overland flow that lasted for at least 10 min and had flow depths ranging between 1 and 5 mm.

Figure 6

3.3 Evaluation of impact-based classification

The proposed impact-based classification method was evaluated for all three stations, respectively, with Würzburg station shown as an example (Fig. 4b, Tab. 2). The three-dimensional (3D) scatterplot in Figure 4b shows that only certain quadrants of the plots contained rainfall events that generated overland flow, with a high concentration appearing in the first quadrant (duration: < 5 h, mean intensity: < 5 mm/10 min). While 867 events met at least the criterion of class 1 (flow depth df >= 1 mm/10 min), only 14 events generated an overland flow of at least 4 mm in 10 min (class 4, see Tab. 2). Classes 1 and 2 included events of both short and long durations (ranging from 10 min to 22.4 h), whereas events in classes 3 and 4 were generally much shorter, with durations up to seven hours.

The associated mean and peak intensities of the rainfall events increased from class 1 to 4 and the spans of the intensities became considerably larger with increasing class numbers (e.g. maximum intensity for class 1: 0.9 – 2.7 mm/10 min, class 4: 8.4 – 29 mm/10 min, Tab. 2). There was only a small degree of overlap between the four classes with regard to maximum intensity, but there was substantial overlap between the mean intensity and rainfall amount. Figure 4b clearly shows that using only peak intensities to describe the magnitude of impact cannot adequately reflect the complexity of runoff responses, particularly for class 3 and 4 events. In contrast, it appears necessary to include all information available for the delineated rainfall model to classify the resulting impacts accordingly. The proposed classification of rainfall events based on simulating overland flow behaviour fills this gap by including the entire sequence of individual rainfall events.

To illustrate the potential of the proposed impact-based classification method, it was compared to a conventional method after the DWD (n.d. a, b, Tab. 3), which uses rainfall intensity as the only classification parameter. The DWD classification scheme categorises rainstorms into three severity levels and includes intensity thresholds for 10 min, one and six hours, but only for the highest severity level storm durations below one hour are considered. In this comparison, we only used the highest DWD severity level (as summarised in Tab. 3), as otherwise, the comparison would be statistically flawed. Using the DWD categorisation, 33 events were categorised as extreme events for the station Würzburg (Tab. 2); in comparison, 91 and 14 events were assigned to our high-impact classes 3 and 4, respectively. The scatterplots in Figure 7 show that not all DWD extreme events were detected in class 4 by the impact-based approach, but more than half of them were assigned to class 3. There appears to be more consistency between the impact-based and the conventional method in event identification for longer storm durations, whereas for shorter durations below one hour, a much larger spectrum of equally extreme events is identified by the impact-based method.

Table2

Table3

Figure 7

4 Application of the rainfall classification method for impact-based time-series analysis

The classification method described and evaluated here was used for an impact-based time-series analysis of rainstorm events, which we examined at both seasonal and annual scales (Figs. 8 and 9) for three example urban stations on a north–south transect across Germany (Hamburg, Potsdam, Würzburg).

Rainfall events generating relevant overland flow (by our definition, class 1 – 4) occurred throughout the year, with the number of events decreasing considerably with increases in the threshold for flow depth/10 min, ultimately being limited to the summer season (May – September) (Fig. 8).

Up to 50% of all rainfall events in summer generated overland flow, of which 60 – 80% was due to events in class 1 and 20 – 40% of class 2 – 4 (Fig. 8). With very few exceptions, class 4 events occurred between May and September in Hamburg, and between June and August in Potsdam and Würzburg. In winter, only approximately 7 – 20% of the monthly rainfall events generated substantial overland flow (mainly class 1).

The mean annual number of rainstorms with significant impacts varied between 40 for Hamburg and 28 for Würzburg and Potsdam, of which, on average, 67% were from class 1, 18% from class 2, 9% from class 3, and 6% from class 4 (Fig. 9).

The greatest number of rainstorm events classified annually (48 – 58) was detected in 2007, while the fewest events were detected in 1995 for Hamburg (19) and 2018 for Potsdam (14) and Würzburg (18).

Over a period of 31 years, no significant annual trends were observed in the total number of rainfall events or rainfall events of individual classes. However, a decadal comparison (1990 – 1999, 2000 – 2009 and 2010 – 2019) showed a substantial increase in rainstorm impacts: In Hamburg, the number of class 4 events increased from 13 to 25 to 31, while those of class 3 events increased from 10 to 29 to 39 per decade. In Würzburg, the number of class 3 events increased from 24 to 32 to 35 per decade, though no increase was detected for class 4 events. Potsdam Station was not considered for decadal comparison due to missing data).

Our classification method provided new insights into the similarities and dissimilarities of different time series regarding the temporal distribution of rainstorm impacts. The next step in analysis will include a systematic review of multiple stations and, where possible, for longer time series; however, the latter will necessarily be limited because of the lack of high-resolution series that extend for longer than 30 years.

Figure 8

Figure 9

5 Discussion

The primary purpose of this study was to present a new impact-based rainstorm classification method to complement the current classification of heavy rainstorms. The proposed method can be readily applied to high-resolution rainfall series, and we showcased its ability to filter events according to rainfall impacts in order to analyse seasonal and annual variations in rainfall intensity.

We also explained the necessity of the new classification approach by the fact that conventional classification approaches (as used by (Haacke and Paton 2021; Hofstätter et al. 2017; Jacobeit et al. 2017; Lorenz et al. 2019) normally only characterise the severity of rainstorm events based on averaged values, such as the total amount of rainfall or maximum intensity of fixed time intervals. Additionally, conventional classifications employ hourly or daily resolutions, even though higher-resolution data are often locally available. However, the use of aggregated rainfall data poses a risk of mischaracterising the impacts of rainfall events. The 3D-scatterplots of classified events (Fig. 4b) demonstrated that those with very similar rainstorm characteristics were assigned to different impact classes, supporting the need to include more temporal dynamics when evaluating rainstorms. Furthermore, the comparison between a conventional method and the proposed method showed that using rainfall intensities as a classification parameter only is not sufficient to describe an events impact. A better representation of rainstorm characteristics was achieved by our approach, considering both the intermittency of rainfall and the entire course of individual rainfall events, thus enabling the precise computation of the flow depth profile, which ultimately allows events to be classified according to their impacts.

However, using high-resolution data is a limiting factor for the applicability of the proposed method as they are often not available in all regions. Data sets covering a short period of a few years can still be used for an initial assessment, but data for at least 30 years is strongly recommended for time series analysis. Although our approach can be adapted to data of coarser resolution (e.g. hourly data), we would not recommend this as the presentation of extreme events will be skewed. Furthermore, the four impact classes were derived for the three selected stations in Germany and might need to be adapted for stations elsewhere.

Our approach includes several uncertainties, which we addressed in the evaluation of the three classification steps: event delineation, overland flow computation, and event-based classification. First, event delineation depends on the choice of IET, which needs to be adjusted to regional rainfall patterns, as discussed by Dunkerely (2010) and Duque (2020). Second, higher-resolution (e.g. 1 min) rainfall data may be employed, which will result in a better reproduction of overland flow hydrography and may cause in higher peak flow depths for extreme rainfall intensities. Third, our default setting of 10 min, for which a rain event generated and sustained a certain overland flow depth, was arbitrary to some extent, and it was deemed to represent a reasonable baseline for the on-set of pluvial flooding and pollution transfer, but regional characteristics might necessitate changes to this time setting.

Finally, our classification relies on a simplification of a sealed, typical urban surface for which the overland flow model was parameterised using fixed values for slope, infiltration rate, interception, and depression storage, and antecedent moisture conditions were neglected. No runoff concentration, which is normally associated with pluvial flooding and pollution transfer, was modelled, but only overland flow was generated on the model surface. This approach accounts for the micro-topography of sealed surfaces by including interception and depression storage, as experimentally quantified by Nehls et al. (2015) and Rammal and Berthier (2020).

A more realistic, but also more complex representation of urban surfaces would include the reproduction of the meso-topography of street surfaces such as kerbside features and larger depressions and drain channels or the reproduction of entire street canyon features (GebreEgziabher and Demissie 2020; Li et al. 2008; Xing et al. 2019). The latter model surface would require the definition of multiple typical street canyon types for different city structures. By doing this, runoff concentrations could be reproduced much more accurately, and the actual impact of pluvial flooding for all delineated rainfall events could be quantified more accurately. At the same time, different street canyon types will result in different impact-based rainfall classifications. A supra-regional analysis of rainfall characteristics, as carried out here for the simplified urban surface for Hamburg, Potsdam and Würzburg, would not be feasible any more, as too many very different canyon types would need to be considered simultaneously. We therefore suggest keeping the overland flow model simplistic for analysing general behavioural trends in extremes; however, one may want to consider using a much more complex representation of urban layouts when preparing rainfall classifications for regional studies or individual cities.

6 Conclusions

Up to this point, extreme rainfalls were merely categorised based on their maximum rainfall intensity, amount or return period. We proposed a new classification method for extreme rains that used their potentials to generate overland flow on a typical urban asphalt surface as a filter to categorise their extremeness. Besides the maximum rainfall intensity, this approach considers the full dynamics of the rainstorm event including actual length of rainfall events and other characteristics such as precipitation amount, mean intensity and flow depths.

The evaluation of this method including a comparison with a conventional classification method showed that it is appropriate to use flow depth per time as an indicator of the generated impacts of overland flow in order to classify rainfall events. Rainfall events generating substantial overland flow were assigned to several impact classes indicating increasing flow depths and thus stronger impact. We found that events with similar rainstorm intensities were assigned to different impact classes. This observation supports the assumption of a higher risk of misjudging the impact of events based on rainstorm intensities alone. Therefore, improved characterisation and classification of rainfall events can be achieved using the approach proposed here. In a further step, a temporal analysis was carried out for all four classes for three different locations in Germany. Results showed that events with the greatest impacts mainly occurred in summer, and there was a clear increase in the number of events over the last three decades.

However, this method is limited by its need of high-resolution data. Furthermore, flow depth distributions may vary for other regions or other surface layouts so that impact classes may need adaptation. Further analysis may include the analysis of spatial variations as well as the investigation of surface characteristics and varying class thresholds.

Acknowledgments:

This work was supported by the Deutsche Forschungsgemeinschaft as part of the research training group Urban Water Interfaces (GRK 2032/2).

Funding details. This work was supported by the Detusche Forschungsgemeinschaft (DFG) under Grant [GRK 2032/2].

Disclosure statement. The authors report there are no competing interests to declare.

Data availability statement. All data, models, and code generated or used during the study appear in the submitted article.

References

Abrahams, A. D., Li, G., Krishnan, C., & Atkinson, J. F., 1998. "Predicting sediment transport by interrill overland flow on rough surfaces." *Earth Surface Processes and Landforms* 23: 1087–1099.

Acero, F. J., García, J. A., & Gallego, M. C., 2011. "Peaks-over-Threshold Study of Trends in Extreme Rainfall over the Iberian Peninsula." *Journal of Climate* 24(4): 1089–1105. doi:10.1175/2010JCLI3627.1.

Adams, B. J., & Papa, F., 2000. *Urban Stormwater Management Planning with Analytical Probabilistic Models*. New York: John Wiley & Sons.

Agilan, V., Umamahesh, N. V., & Mujumdar, P. P., 2021. "Influence of threshold selection in modeling peaks over threshold based nonstationary extreme rainfall series." *Journal of Hydrology* 593: 125625. doi:10.1016/j.jhydrol.2020.125625.

Anagnostopoulou, C., & Tolika, K., 2012. "Extreme precipitation in Europe: Statistical threshold selection based on climatological criteria." *Theoretical and Applied Climatology* 107(3–4): 479–489. doi:10.1007/s00704-011-0487-8.

Balstrøm, T., & Crawford, D., 2018. Arc-Malstrøm: "A 1D hydrologic screening method for stormwater assessments based on geometric networks." *Computers & Geosciences* 116: 64–73. doi:10.1016/j.cageo.2018.04.010.

Beguería, S., Angulo-Martínez, M., Vicente-Serrano, S. M., López-Moreno, J. I., & El-Kenawy, A., 2011. "Assessing trends in extreme precipitation events intensity and magnitude using non-stationary peaks-over-threshold analysis: A case study in northeast Spain from 1930 to 2006." *International Journal of Climatology*, 31(14): 2102–2114. doi:10.1002/joc.2218.

Brieber, A., & Hoy, A., 2019. "Statistical analysis of very high-resolution precipitation data and relation to atmospheric circulation in Central Germany." *Advances in Science and Research* 16: 69–73. doi:10.5194/asr-16-69-2019.

Climate Data Center., 2021. *CDC-Portal*. Deutscher Wetterdienst. https://opendata.dwd.de/.

DWD (Deutscher Wetterdienst). n.d. (a). *Wetter- und Klimalexikon: Niederschlagsintensität*. Accessed Januar 20, 2022. https://www.dwd.de/DE/service/lexikon/Functions/glossar.html?lv2=101812&lv3=101906

DWD (Deutscher Wetterdienst). n.d. (b). *Wetter- und Klimalexikon: Starkregen*. Accessed Januar 20, 2022. https://www.dwd.de/DE/service/lexikon/Functions/glossar.html?nn=103346&lv2=102248&lv3=102572.

DHI., 2000. *MOUSE Surface Runoff Models—Reference Manual*. DHI Water & Environment.

Di Salvo, C., Ciotoli, G., Pennica, F., & Cavinato, G. P., 2017. "Pluvial flood hazard in the city of Rome (Italy)." *Journal of Maps* 13(2): 545–553. doi:10.1080/17445647.2017.1333968.

Dunkerley, D., 2008. "Identifying individual rain events from pluviograph records: A review with analysis of data from an Australian dryland site." *Hydrological Processes* 22(26): 5024–5036. doi:10.1002/hyp.7122.

Dunkerley, D., 2017. "An approach to analysing plot scale infiltration and runoff responses to rainfall of fluctuating intensity: Plot Scale Infiltration." *Hydrological Processes* 31(1): 191–206. doi:10.1002/hyp.10990.

Dunkerley, D., 2020. "Rainfall intensity in geomorphology: Challenges and opportunities." *Progress in Physical Geography: Earth and Environment* 45(4): 488-513. doi:10.1177/0309133320967893.

Dunkerley, D. L., 2010. "How do the rain rates of sub-event intervals such as the maximum 5- and 15-min rates (I5 or I30) relate to the properties of the enclosing rainfall event?" *Hydrological Processes* 24(17): 2425–2439. doi:10.1002/hyp.7650.

Duque, L. F., 2020. *Inter-Event Time Definition (package 'IETD')* (S. 9). https://cran.r-project.org/web/packages/IETD/index.html.

Fang, N.-F., Shi, Z.-H., Li, L., Guo, Z.-L., Liu, Q.-J., & Ai, L., 2012. "The effects of rainfall regimes and land use changes on runoff and soil loss in a small mountainous watershed." *CATENA* 99: 1–8. doi:10.1016/j.catena.2012.07.004.

Forzieri, G., Bianchi, A., Silva, F. B. e, Marin Herrera, M. A., Leblois, A., Lavalle, C., Aerts, J. C. J. H., & Feyen, L., 2018. "Escalating impacts of climate extremes on critical infrastructures in Europe." *Global Environmental Change* 48: 97–107. doi:10.1016/j.gloenvcha.2017.11.007.

Gaál, L., Molnar, P., & Szolgay, J., 2014. "Selection of intense rainfall events based on intensity thresholds and lightning data in Switzerland." *Hydrology and Earth System Sciences* 18(5): 1561–1573. doi:10.5194/hess-18-1561-2014.

GebreEgziabher, M., & Demissie, Y., 2020. "Modeling Urban Flood Inundation and Recession Impacted by Manholes." *Water* 12(4): 1160. doi:10.3390/w12041160.

Haacke, N., & Paton, E. N., 2021. "Analysis of diurnal, seasonal and annual variability of urban sub-hourly to hourly rainfall extremes in Germany." *Hydrology Research* 52(2): 478–491. doi:10.2166/nh.2021.181.

Hofstätter, M., Lexer, A., Homann, M., & Blöschl, G., 2017. "Large-scale heavy precipitation over central Europe and the role of atmospheric cyclone track types." *International Journal of Climatology* 38(S1): 497-517. doi:10.1002/joc.5386.

Innovyze. (2020). *InfoWorks ICM* (10.5) [Computer software]. https://www.innovyze.com/en-us/products/infoworks-ws-pro.

Jacobeit, J., Homann, M., Philipp, A., & Beck, C., 2017. "Atmospheric circulation types and extreme areal precipitation in southern central Europe." *Advances in Science and Research* 14: 71–75. doi:10.5194/asr-14-71-2017.

Jacobs, J. M., Cattaneo, L. R., Sweet, W., & Mansfield, T., 2018. "Recent and Future Outlooks for Nuisance Flooding Impacts on Roadways on the U.S. East Coast." *Transportation Research Record: Journal of the Transportation Research Board* 2672(2): 1–10. doi:10.1177/0361198118756366.

Jo, E., Park, C., Son, S.-W., Roh, J.-W., Lee, G.-W., & Lee, Y.-H., 2020. "Classification of Localized Heavy Rainfall Events in South Korea." *Asia-Pacific Journal of Atmospheric Sciences* 56(1): 77–88. doi:10.1007/s13143-019-00128-7.

Li, X.-X., Leung, D. Y. C., Liu, C.-H., & Lam, K. M., 2008. "Physical Modeling of Flow Field inside Urban Street Canyons." *Journal of Applied Meteorology and Climatology* 47(7): 2058–2067. doi:10.1175/2007JAMC1815.1.

Lorenz, J. M., Kronenberg, R., Bernhofer, C., & Niyogi, D., 2019. "Urban Rainfall Modification: Observational Climatology Over Berlin, Germany." *Journal of Geophysical Research: Atmospheres* 124(2): 731–746. doi:10.1029/2018JD028858.

Moftakhari, H. R., AghaKouchak, A., Sanders, B. F., Allaire, M., & Matthew, R. A., 2018. "What Is Nuisance Flooding? Defining and Monitoring an Emerging Challenge." *Water Resources Research* 54(7): 4218–4227. doi:10.1029/2018WR022828.

Moftakhari, H. R., AghaKouchak, A., Sanders, B. F., & Matthew, R. A., 2017. "Cumulative hazard: The case of nuisance flooding." *Earth's Future* 5(2): 214–223. doi:10.1002/2016EF000494.

Nehls, T., Menzel, M., & Wessolek, G., 2015. "Depression Storage Capacities of Different Ideal Pavements as Quantified by a Terrestrial Laser Scanning- Based Method." *Water Science & Technology* 71(6): 862-9. doi:10.2166/wst.2015.025.

Parsons, A. J., & Stromberg, S. G. L., 1998. "Experimental analysis of size and distance of travel of unconstrained particles in interrill flow." *Water Resources Research* 34(9): 2377–2381. doi:10.1029/98WR01471.

Paton, E., & Haacke, N., 2021. "Merging patterns and processes of diffuse pollution in urban watersheds: A connectivity assessment." *WIREs Water* 8(4): e1525. doi:10.1002/wat2.1525.

R Core Team., 2020. *R: A Language and Environment for Statistical Computing.* R Foundation for Statistical Computing. https://www.R-project.org.

Rammal, M., & Berthier, E., 2020. "Runoff Losses on Urban Surfaces during Frequent Rainfall Events: A Review of Observations and Modeling Attempts." *Water* 12(10): 2777. doi:10.3390/w12102777.

Restrepo-Posada, P. J., & Eagleson, P. S., 1982. "Identification of independent rainstorms." *Journal of Hydrology* 55(1–4): 303–319. doi:10.1016/0022-1694(82)90136-6.

Rossman, L. A., 2004. *Storm Water Management Model User's Manual Version 5.0*. U.S. Environmental Protection Agency, Washington, DC, EPA/600/R-05/040.

Rözer, V., Peche, A., Berkhahn, S., Feng, Y., Fuchs, L., Graf, T., Haberlandt, U., Kreibich, H., Sämann, R., Sester, M., Shehu, B., Wahl, J., & Neuweiler, I., 2021. "Impact-Based Forecasting for Pluvial Floods." *Earth's Future* 9(2). doi:10.1029/2020EF001851.

Salvadore, E., Bronders, J., & Batelaan, O., 2015. "Hydrological modelling of urbanized catchments: A review and future directions." *Journal of Hydrology* 529: 62–81. doi:10.1016/j.jhydrol.2015.06.028.

Schär, C., Ban, N., Fischer, E. M., Rajczak, J., Schmidli, J., Frei, C., Giorgi, F., Karl, T. R., Kendon, E. J., Tank, A. M. G. K., O'Gorman, P. A., Sillmann, J., Zhang, X., & Zwiers, F. W., 2016. "Percentile indices for assessing changes in heavy precipitation events." *Climatic Change* 137(1–2): 201–216. doi:10.1007/s10584-016-1669-2.

Scoging, H., 1992. "Modelling overland-flow hydrology for dynamic hydraulics." Chap. 5 in *Overland Flow. Hydraulics and Erosion Mechanics*. London and New York: Routledge.

Sen, S., Srivastava, P., Dane, J. H., Yoo, K. H., & Shaw, J. N., 2010. "Spatial–temporal variability and hydrologic connectivity of runoff generation areas in a North Alabama pasture—Implications for phosphorus transport." *Hydrological Processes* 24(3): 342–356. doi:10.1002/hyp.7502.

Suarez, P., Anderson, W., Mahal, V., & Lakshmanan, T. R., 2005. "Impacts of flooding and climate change on urban transportation: A systemwide performance assessment of the Boston Metro Area." *Transportation Research Part D: Transport and Environment* 10(3): 231–244. doi:10.1016/j.trd.2005.04.007.

Wenzel, H. G., & Voorhees, M. L., 1981. *Evaluation of the urban design storm concept*. Final report, Water Resources Center, Report No. 164. https://www.ideals.illinois.edu/handle/2142/90287.

Westra, S., Fowler, H. J., Evans, J. P., Alexander, L. V., Berg, P., Johnson, F., Kendon, E. J., Lenderink, G., & Roberts, N. M., 2014. "Future changes to the intensity and frequency of short-duration extreme rainfall." *Reviews of Geophysics* 52(3): 522–555. doi:10.1002/2014RG000464.

Xing, Y., Liang, Q., Wang, G., Ming, X., & Xia, X., 2019. "City-scale hydrodynamic modelling of urban flash floods: The issues of scale and resolution." *Natural Hazards* 96(1): 473–496. doi:10.1007/s11069-018-3553-z.

Yoo, C., & Park, C., 2012. "Comparison of Annual Maximum Rainfall Series and Annual Maximum Independent Rainfall Event Series." *Journal of Korea Water Resources Association* 45(5): 431–444. doi:10.3741/JKWRA.2012.45.5.431.

Yuan, X., Zheng, N., Ye, F., & Fu, W., 2019. "Critical runoff depth estimation for incipient motion of non-cohesive sediment on loose soil slope under heavy rainfall." *Geomatics, Natural Hazards and Risk* 10(1): 2330–2345. doi:10.1080/19475705.2019.1697760.

Tables

Table 1. Typical parameterisation of a street surface.

Parameter	Values
Slope (*s*)	2.5 %
Friction factor (*ff*)	0.1
Infiltration rate (*i*)	0.36 mm/h (Nehls et al. 2015)
Interception and depression storage (*loss*)	0.46 mm (Rammal and Berthier 2020)

Table 2. Classification of the delineated rainfall events for Würzburg Station from 1990 – 2020.

Traits	Class 1	Class 2	Class 3	Class 4	DWD
Threshold [mm/10min]	1	2	3	4	
Impact level	low	middle	high	very high	extreme rainfall
Number of events (%)	590 (19.9)	172 (5.8)	91 (3.1)	14 (0.47)	33 (1.1)
Event duration [min and longest in h]	10 – 1350 (22.4h)	10 – 1210 (20.2h)	10 – 410 (6.8h)	10 – 350 (5.8h)	10 – 360 (6h)
Precipitation amount [mm]	1.6 – 56.2	2.8 – 51.3	4.9 – 47.0	18.7 – 69.6	8.7 – 69.6
Maximum intensity [mm/10min]	0.91 – 2.7	2.5 – 4.5	4.5 – 13.1	8.4 – 29.0	8.3 – 29.0
Mean intensity [mm/10min]	0.1 – 2.7	0.2 – 4.1	0.4 – 11.5	1.2 – 23.2	0.7 – 23.2

Table 3. Extreme rainfall events and their threshold values according to DWD (n.d. a, b).

Time-resolution	Rainfall intensity
10 min	≥ 8.3 mm
60 min (1h)	≥ 40 mm
360 min (6h)	≥ 60 mm

Figures

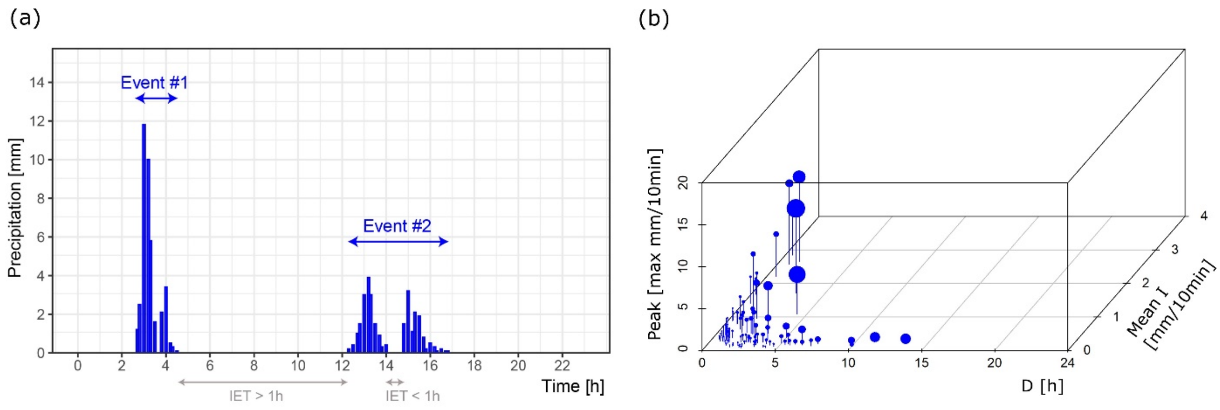

Figure 1. (a) Schematic showing the identification of individual rainfall events. (b) Delineated rainfall events in 2010 for the station Würzburg. Point sizes represent precipitation amounts.

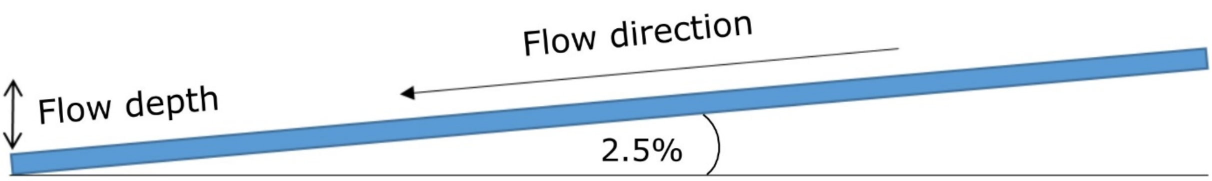

Figure 2. Schematic representation of the model street.

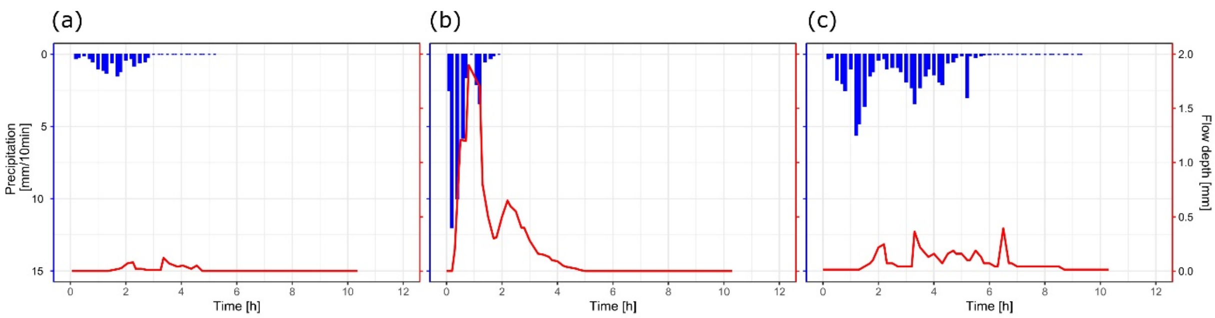

Figure 3. Example flow depth dynamics of three rainfall types: (a) drizzle, (b) convective, and (c) continuous rainfall.

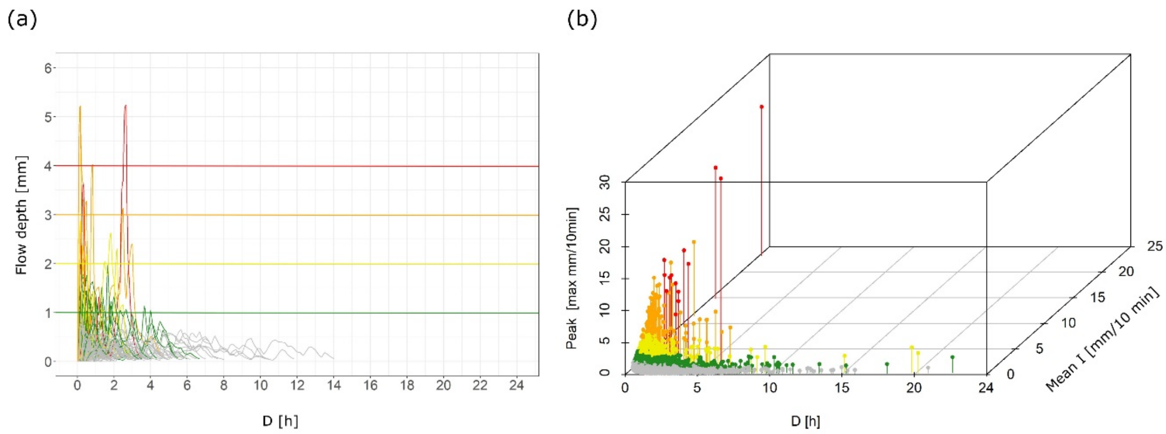

Figure 4. (a) Flow depths dynamics of multiple delineated rainfall events; (b) classification of rainfall events corresponding to flow depth categories in a three-dimensional scatterplot (output for Würzburg). Colour coding: grey: events generating no overland flow, green: class 1, yellow: class 2, orange: class 3, red: class 4 (see Tab. 2 for threshold values).

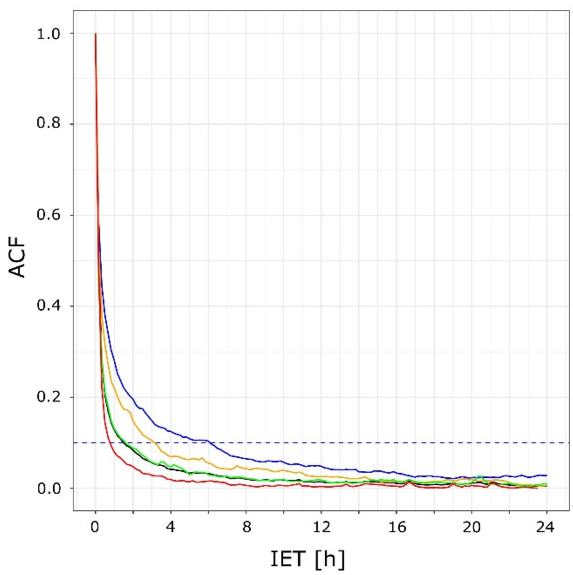

Figure 5. Output of the autocorrelation analysis (AutoA method) for Würzburg station for the whole period (1990 – 2020) and all four seasons. The x-axis is in 10 min time steps. Abbreviations: ACF: autocorrelation function. Lines show the mean of ACF for 1990 – 2020 (black), summer (June – August; red), autumn (September – November; orange), winter (December – February; blue), and

spring (March – May; green). The dashed horizontal line is the critical correlation for a significance level of 10%.

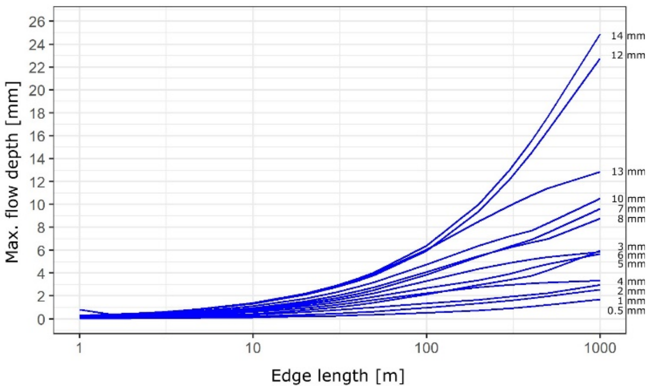

Figure 6. Development of flow depths with increasing model domain. Each line represents a single rainfall event. Events were chosen with regard to peak intensity, which ranged between 1 and 14 mm/10min.

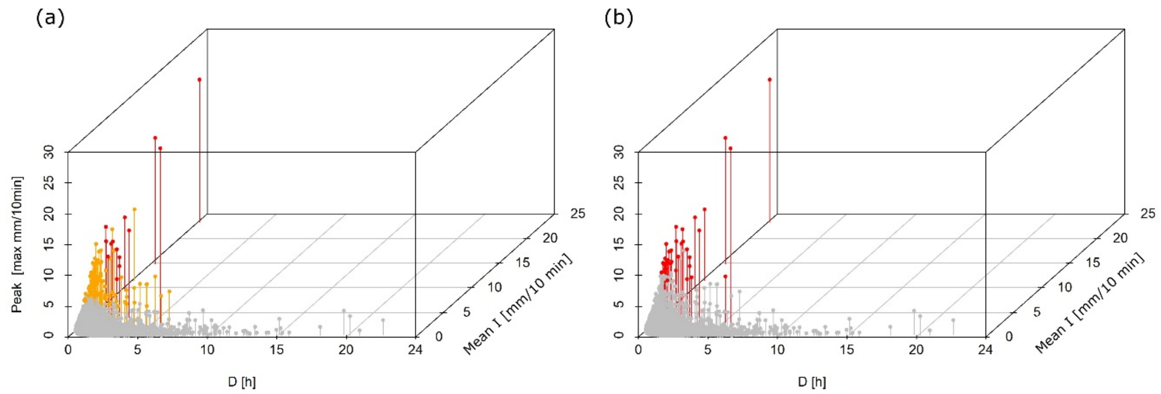

Figure 7. Comparison of detected extreme events between (a) the proposed impact-based classification method (red: events of class 4, orange: events of class 3, grey: all other events), and (b) a conventional classification method using rainfall intensity thresholds (red: events selected by using thresholds according to Tab. 3, grey: all other events).

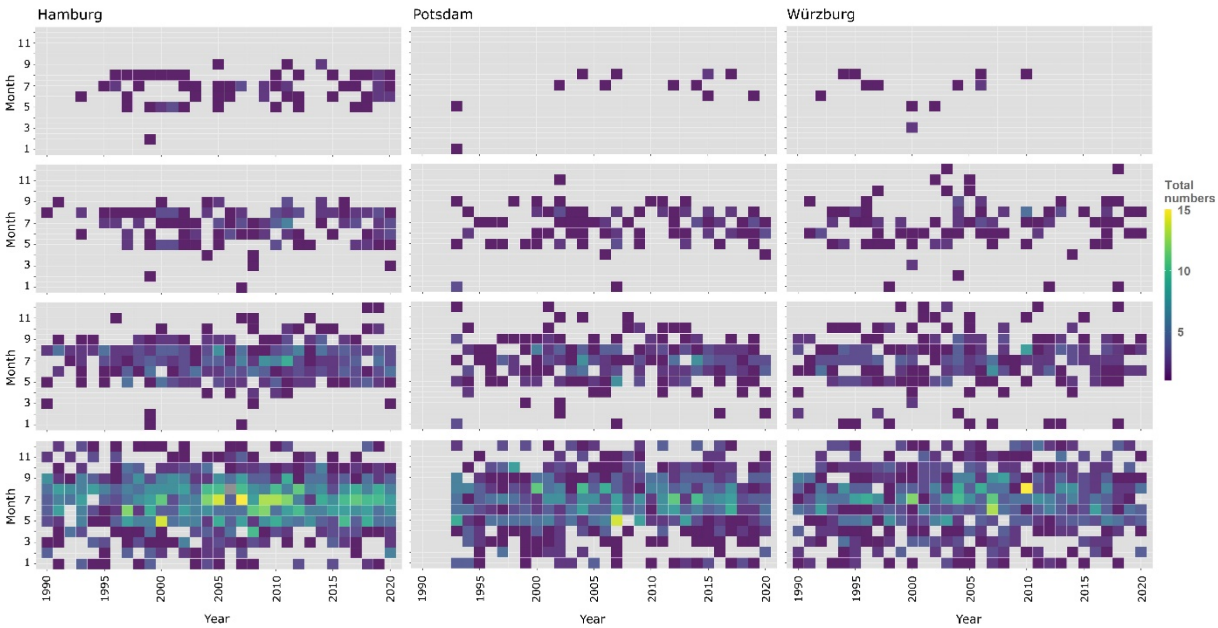

Figure 8. Seasonal rainfall frequency distribution of class 4 (first row), class 3 (second row), class 2 (third row), and class 1 (fourth row) events in Würzburg, Hamburg, and Potsdam.

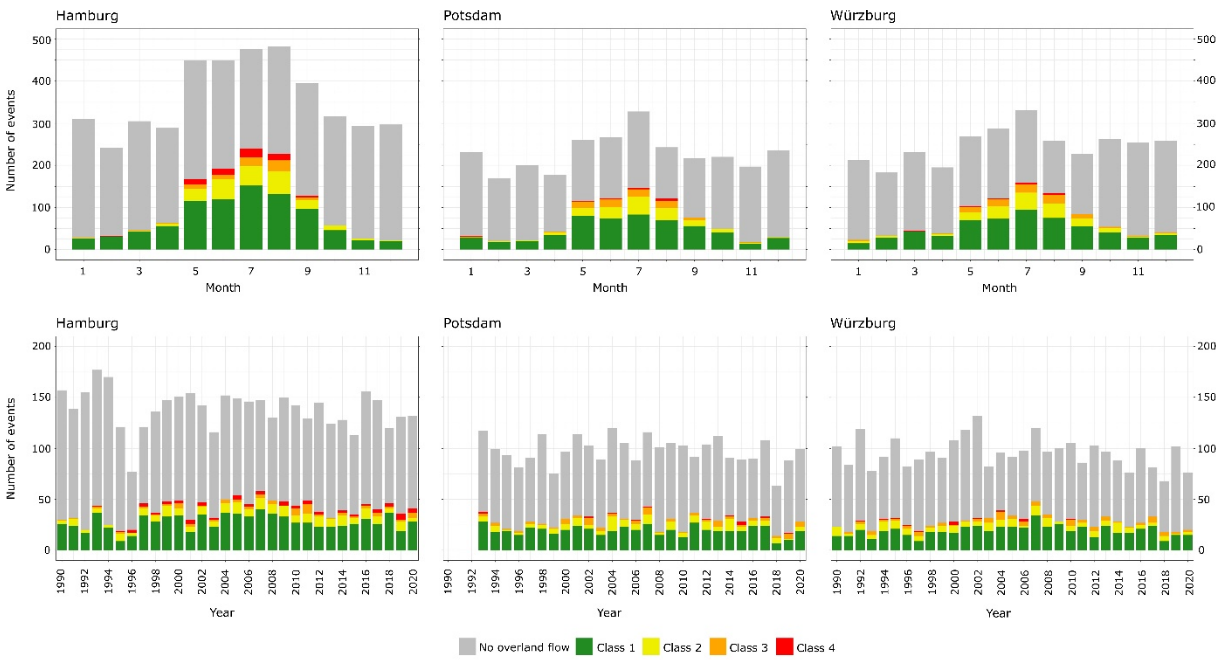

Figure 9. Seasonal (first row) and annual (second row) number of classified storm events for a period of 31 years for Würzburg and Hamburg (1990 – 2020) and for 28 years for Potsdam (1993 – 2020). Colours show events of classes with: no overland flow (grey), class 1 (green), class 2 (yellow), class 3 (orange), and class 4 (red, see Tab. 2 for thresholds).